tvst

Lens

Comparative Analysis of Optical Quality of Monofocal, Enhanced Monofocal, Multifocal, and Extended Depth of Focus Intraocular Lenses: A Mobile Model Eye Study

Eun Chul Kim[1], Soo Yeon Cho[1], Ji Eon Kang[1], Gahee Nam[1], Young Chae Yoon[1], Woong-Joo Whang[1], Kyung-Sun Na[1], Hyun-Seung Kim[1], and Ho Sik Hwang[1]

[1] Department of Ophthalmology, College of Medicine, The Catholic University of Korea, Seoul, Republic of Korea

Correspondence: Ho Sik Hwang, Department of Ophthalmology, Yeouido St. Mary's Hospital, The Catholic University of Korea, 10, 63-ro, Yeongdeungpo-gu, Seoul 07345, Republic of Korea.
e-mail: huanghs@catholic.ac.kr

Received: July 20, 2022
Accepted: April 15, 2023
Published: July 5, 2023

Keywords: multifocal; intraocular lens; model eye; halo; defocus curve

Citation: Kim EC, Cho SY, Kang JE, Nam G, Yoon YC, Whang WJ, Na KS, Kim HS, Hwang HS. Comparative analysis of optical quality of monofocal, enhanced monofocal, multifocal, and extended depth of focus intraocular lenses: A mobile model eye study. Transl Vis Sci Technol. 2023;12(7):5, https://doi.org/10.1167/tvst.12.7.5

Purpose: To use the revised model eye to observe and compare how the world is perceived by patients with monofocal intraocular lens (IOL), Eyhance, bifocal IOL, and Symfony, and check its performance.

Methods: The new mobile model eye consists of an artificial cornea, an IOL, a wet cell, an adjustable lens tube, a lens tube, an objective lens, a tube lens, and a digital single-lens reflex camera. We collected photographs of distant buildings and streets at night, videos of the focusing process, and videos of United States Air Force resolution target from 6 m to 15 cm and analyzed them quantitatively.

Results: In this revised model eye using an objective lens, an artificial cornea similar to the human cornea could be used. Using a digital single-lens reflex camera, high-resolution imaging was possible without an additional computer. Fine focusing was possible using an adjustable lens tube. For monofocal IOL, the contrast modulation was 0.39 at 6 m and decreased consistently. It was nearly 0 as the model eye got closer than 1.6 m. For Eyhance, the contrast modulation was 0.40 at 6 m. It then decreased and increased again. At 1.3 m, it was 0.07 and then decreased again. For Symfony, the contrast modulation was 0.18 at 6 m. Symfony showed the characteristics of a bifocal IOL with low add diopter. Halos (234 pixels) were observed around lights, although smaller than those seen with bifocal IOL (432 pixels).

Conclusions: We could objectively observe and compare how patients with monofocal IOL, Eyhance, bifocal IOL, and Symfony perceived the world using this revised model eye.

Translational Relevance: Data obtained by this new mobile model eye can be used to help patients select their IOLs before cataract surgeries.

Introduction

A mobile model eye was created in our previous study to investigate how patients with multifocal intraocular lenses (IOLs) perceive the world. We inserted monofocal and multifocal IOLs into the model eye and photographed distant buildings during the day, streets at night, and visual acuity charts from a near distance.[1] The buildings that were far were clearly visible with the monofocal IOLs. However, the images with multifocal IOL were slightly hazier than those obtained with monofocal IOL. Halos in night street pictures with multifocal IOL were more intense than those with monofocal IOL. However, the visual acuity chart at a near distance with multifocal IOL was clearer than that with monofocal IOL.

This mobile model eye had some disadvantages. The flange distance (17.526 mm) of the scientific camera used in the study was restricted. Hence, the focal length (f = 300 mm) of the artificial cornea in the model eye was too long compared with the focal length of the human cornea (f = 22.7–25.0 mm).[2] Additionally, the resolution of the camera was very low (1280 × 1024). Because we used a scientific camera, an additional computer was needed to operate the camera. Hence,

its use as a mobile model eye was inconvenient. When focusing, the cornea-IOL complex was moved back and forth in a 30-mm cage, resulting in a method that was rather coarse. Therefore this study revised the previous model eye to overcome these disadvantages.

Recently, in addition to the conventional diffractive bifocal IOL, extended depth of focus lenses and enhanced monofocal IOLs have been developed. Tecnis Symfony (Johnson & Johnson, Santa Ana, CA, USA) is an IOL with an extended range of vision based on diffractive achromatic technology.[3] It has an achromatic diffractive pattern that elongates the focus and compensates for the chromatic aberration of the cornea.[3] Tecnis Eyhance IOL (ICB00) (Johnson & Johnson) is a newly developed monofocal IOL with the same features as those of the ZCB00 IOL, except for the modified aspheric anterior surface of the optic.[4] This enhanced aspheric optic creates a continuous power profile, which is intended to extend the depth of focus. Thus it improves the vision for intermediate tasks compared to a standard monofocal IOL. There are some clinical or experimental studies on these new IOLs.[3–49] However, no reports focus on how the world is perceived by patients with these new IOLs.

Therefore this study uses the revised new mobile model eye to overcome the disadvantages of the previous model. We took photographs showing how the world was perceived by patients with monofocal, Eyhance, bifocal, and Symfony lenses and compared them.

Materials and Methods

A Tecnis monofocal (aspheric, ZCB00; Johnson & Johnson), Eyhance (ICB00; Johnson & Johnson), an enhanced monofocal IOL, a diffractive bifocal (add +3.25 D, ZLB00; Johnson & Johnson), and Symfony (ZXR00; Johnson & Johnson) lenses, which are all one-piece lenses of the same platform from Johnson & Johnson, each with base power +20.0 D were used in this study.

The new mobile model eye was made by revising the previous mobile model eye. The new mobile model eye consists of an artificial cornea (achromatic lens), an IOL, a wet cell, an adjustable lens tube, an objective lens (×10), a tube lens (f = 180 mm), and a digital single-lens reflex (DSLR) camera (D850; Nikon, Tokyo, Japan) (Fig. 1). They were positioned within the 30-mm and 60-mm cage system with four rigid steel rods, thereby eliminating the need for any additional alignment. The image of an external object is focused after passing through the artificial cornea and IOL. It is then focused again on the imaging sensor of the DSLR camera after passing through the objective lens and tube lens. We used an achromatic doublet lens (f = 31.8 mm) (PAC024; Newport, Irvine, CA, USA) as an artificial cornea. This lens is plano-convex design and not aspheric. The radius of curvature is 21.966 mm. Effective focal length is 31.8 mm and optical power is 31.4 D. This lens was made of N-BAF10 (Schott, Mainz, Germany)/N-SF10 (Schott). These are high quality glasses for optics. The abbe number of N-N-BAF10 and N-SF10 are 47.11 and 28.53, respectively. The wet cell has two 0.5-inch diameter windows (thickness = 1 mm, N-BK7). It was filled with 0.9% normal saline. The IOL was held between two lens adapters with a 3.8-or 4.8-mm aperture. The IOL was loaded while checking the IOL concentration using a dissection microscope. The distance between the posterior surface of the artificial cornea (center thickness, 5.35 mm) and the center of the IOL was 6.8 mm.

The artificial cornea and wet cell containing IOL were mounted on an adjustable lens tube to enable fine focusing. The distance between the cornea-IOL

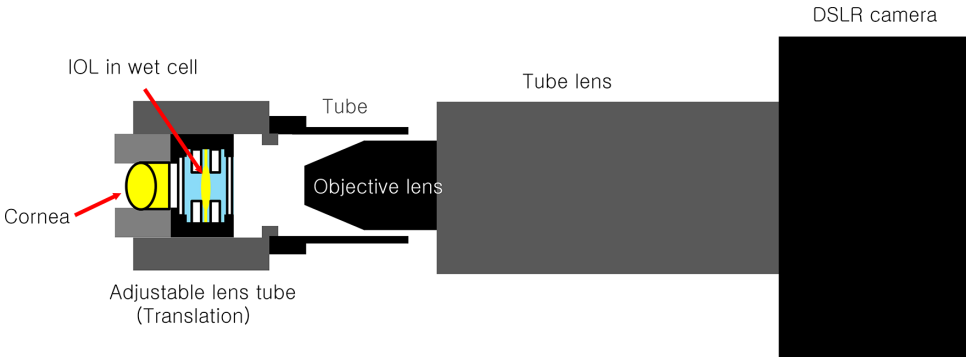

Figure 1. The new mobile model eye. The new mobile model eye consists of an artificial cornea (achromatic lens), an IOL, a wet cell, an adjustable lens tube, a lens tube, an objective lens (×10), a tube lens (f = 180 mm), and a DSLR camera (D850).

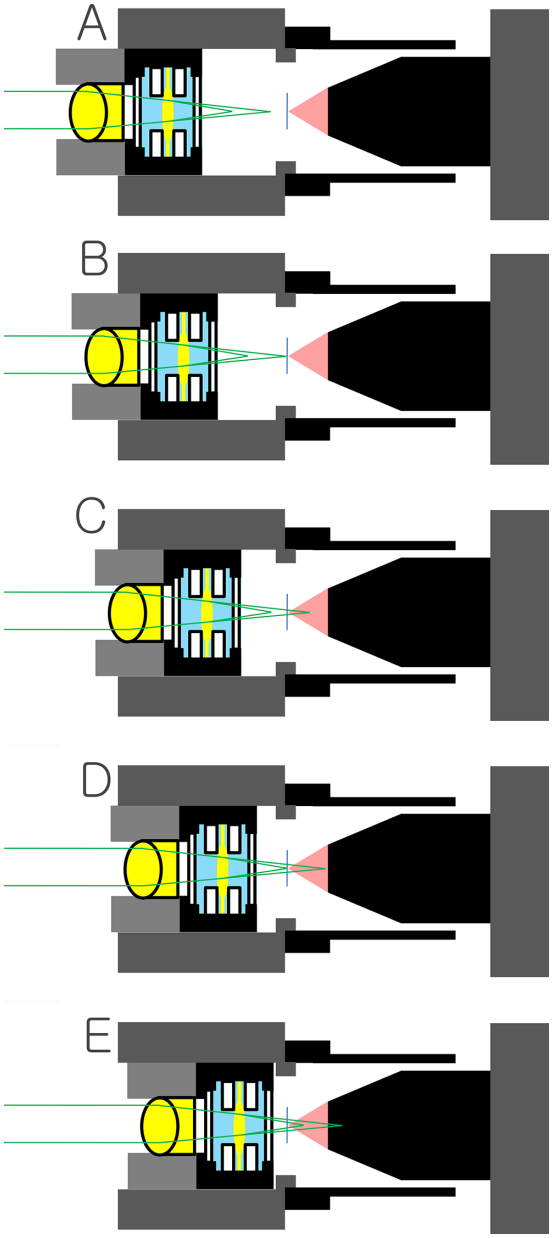

Figure 2. Focusing in case of bifocal IOL. (A) The far and near focus of the bifocal IOL in front of the focal plane of objective lens. (B) The far focus of the bifocal IOL at the focal plane of objective lens. (C) The focal plane of objective lens between far and near focus of the bifocal IOL. (D) The near focus of the bifocal IOL at the focal plane of objective lens. (E) The far and near focus of the bifocal IOL behind the focal plane of objective lens.

complex and the focal plane of the objective lens was finely adjusted by an adjustable lens tube. This adjustable lens tube provides 4.1 mm of linear travel without rotating the cornea-IOL complex mounted in it. This high-precision (1.38 µm/1° rotation) zoom housing provides the ability to accurately control the exact distance between the cornea-IOL complex and objective lens. The ambient light was blocked using a

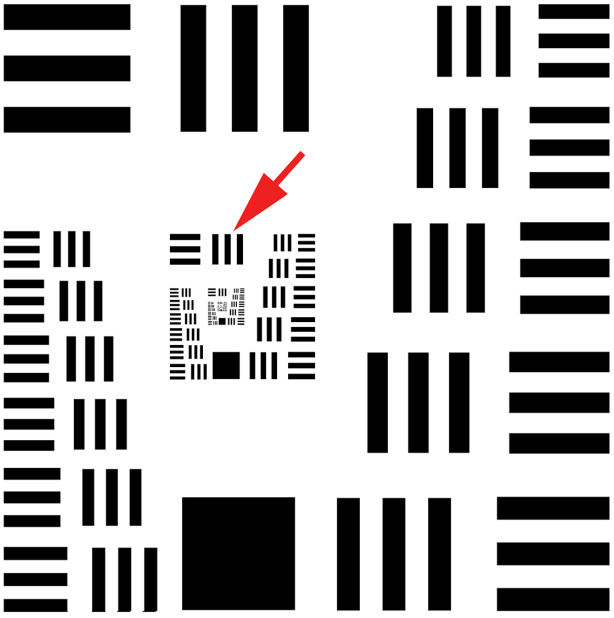

Figure 3. The USAF 1951 resolution test target was used in the study. For quantitative analysis, 0.118 cycles/mm (1 cycle = 8.5 mm) lines (*arrow*) were selected from the resolution target.

lens tube placed between the objective lens and the adjustable lens tube containing the artificial cornea and wet cell. The flange distance of the DSLR camera used in the study was 46.50 mm. We have to use an artificial cornea with longer focal length than that of human cornea (f = 22.7–25.0 mm) and low diopter IOL to focus the image directly on the sensor of the DSLR camera. To overcome this limitation, we used the Olympus lens (Plan N, 10X, 0.25NA; Olympus) as the objective lens. An objective lens can approach closest to the focus, where an external object image forms after passing the cornea and IOL. Therefore the focal length of the artificial cornea could be selected as a value similar to that of a human cornea. The IOL base power could be selected without restriction regardless of the flange distance of the DSLR camera used in the study. Instead, a tube lens (f = 180 mm) had to be mounted in front of the camera. The resolutions of the photo and video obtained using the DSLR camera (Nikon D850) were 8256 × 5504 and 3840 × 2160, respectively. We adjusted the focus and obtained a photograph with the DSLR camera monitor. Hence, no additional computer was required.

The mobile eye was focused on a distant building. In the case of a monofocal IOL, focusing was performed to form the clearest image. For other IOLs, except for monofocal IOLs, accurate focusing is important to check the multifocal function of the multifocal IOLs. In the case of bifocal IOL, Symfony, and Eyhance, the longest focus among two or more foci was set to be located at the camera sensor (Fig. 2B). We

Figure 4. Experiment set up for quantitative analysis. (A) We printed the USAF 1951 resolution test target on 50 cm × 50 cm paper and attached it to a stand panel. Two LED lights (GVM 800D-RGB LED Studio 2-Video Light Kit) were used to illuminate the target at an angle of 45° each. A video of the mobile model eye approaching the target from 6 m to 15 cm was recorded. A dolly track (Glide Gear, Straight Track with Carry Bag [12′]) was installed on the floor for film shooting. A tripod dolly with wheels (Glide gear, tripod dolly SYL-960) was put on the track. A tripod was installed on the tripod dolly. (B) A mobile model eye was installed on the tripod. A tape measure was installed on the floor and inside the dolly track. An additional camera (iPhone 4) was installed on the tripod dolly to record the tape measure on the floor. During the recording, the dolly was pushed as the researcher walked.

used the camera monitor for focusing. The magnification of the camera monitor was appropriately enlarged for fine focusing. Using this revised mobile model eye, the following tests were repeated for monofocal IOL, Eyhance, bifocal IOL, and Symfony. The camera setting and aperture size of all four IOLs were identical in each test.

A Distant Building, Daytime

To check how distant objects are perceived by patients with multifocal IOLs, a distant building (380 m away from our laboratory) was photographed with our mobile model eye. The facade of this building was at an angle of 32° from the axis connecting our laboratory and the center of the building's signboard (Supplementary Fig. S1). We took photographs after setting the focus at the center of the letters on the signboard. The IOLs were held between two lens adapters with a 3.8-mm aperture.

Focusing

The focusing process using an adjustable lens tube while taking photographs of the distant building was recorded as a video. While focusing, the cornea-IOL complex approached the focal plane of the objective lens. Therefore one or several foci passed the focal plane of the objective lens (Fig. 2). The IOLs were held between two lens adapters with a 3.8-mm aperture.

A Distant Building, Nighttime

To check how distant objects are perceived by patients with multifocal IOLs at night, the signboard of the same building was photographed at night. The aperture size of the IOL adapter was set at 4.8 mm to simulate the dilation of the human pupil at night.

A 6 m Distance USAF 1951 Resolution Target

We moved the mobile model eye to check how clearly the resolution target can be perceived at far, intermediate, and near distances through four types of IOLs. It was moved continuously with the IOLs toward the United States Air Force (USAF) 1951 target from 6 m to 15 cm from the target while recording a video. We subsequently quantified the image contrasts at each distance.

To photograph and analyze a resolution target of the same cycles/degree at each distance, the USAF 1951 resolution test target was used (Fig. 3). This

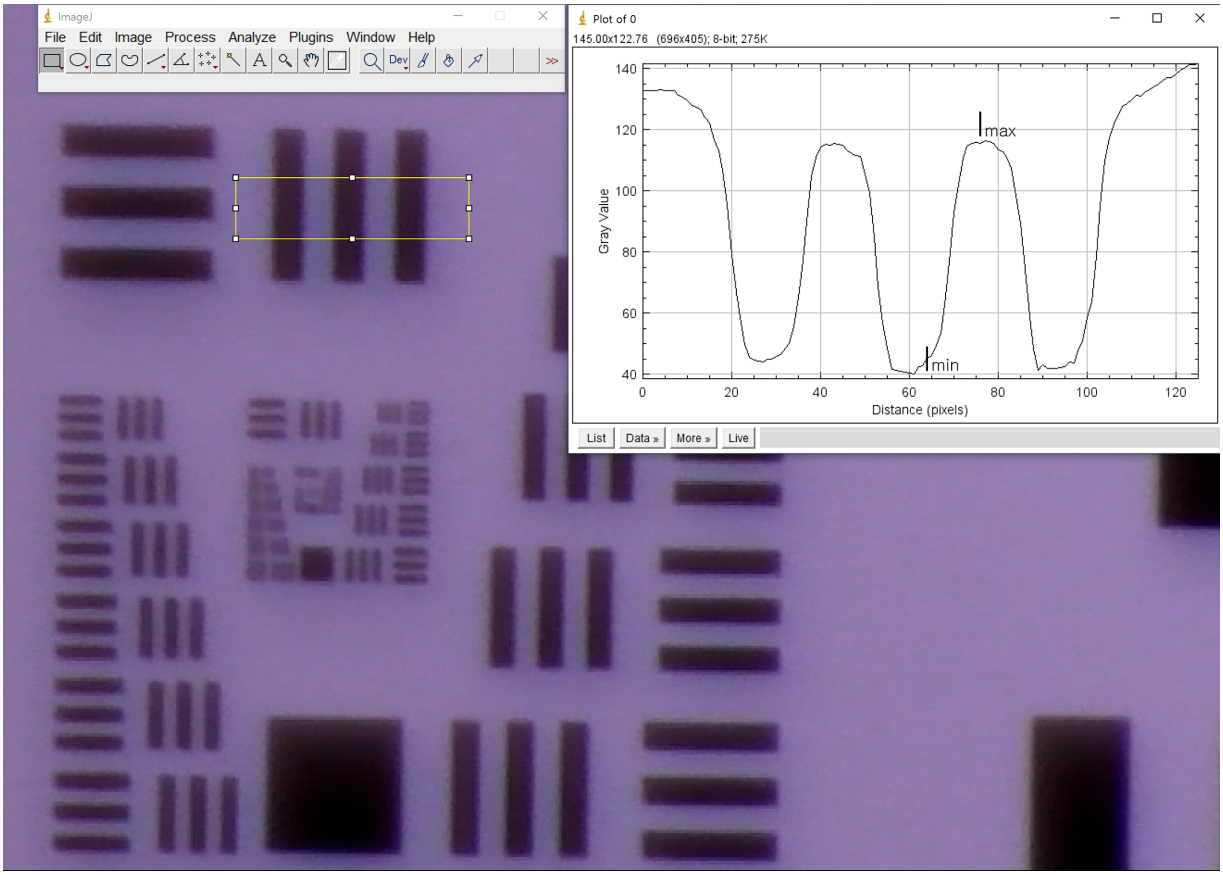

Figure 5. Calculation of contrast modulation of resolution target. Using the ImageJ program, we set a rectangle that crosses the lines, obtained a profile plot, and measured the resolution (contrast modulation) using the following equation. Contrast modulation = $(I_{max} - I_{min})/(I_{max} + I_{min})$.

resolution target has a series of horizontal and vertical lines that are used to determine the resolution of an imaging system. Since the USAF 1951 resolution test target has lines with higher spatial frequency toward the center, we used this as a resolution target. As the mobile model eye approaches a target single spatial frequency line, the lines enlarge in the photographs, and the spatial frequency decreases. Therefore it is impossible to measure the contrast of the resolution target with the same spatial frequency at each distance. We printed the USAF 1951 resolution test target on a 50 cm × 50 cm paper and attached it to a stand panel. Two light-emitting diode (LED) lights (GVM 800D-RGB LED Studio 2-Video Light Kit) were used to illuminate the target at an angle of 45° each (Fig. 4A). We focused the mobile model's eye on a distant building in the abovementioned manner. A video of the mobile model eye approaching the target from 6 m to 15 cm was recorded. A dolly track (Glide Gear, Straight Track with Carry Bag [12′]) was installed on the floor to shoot the video. A tripod dolly with wheels (Glide gear, tripod dolly SYL-960) was put on the track. A tripod was installed on the tripod dolly. A mobile model eye was installed on the tripod (Fig. 4B). The axis of the model eye was adjusted, such that it was exactly parallel to the dolly track and pointed toward the center of the resolution target. A tape measure was installed on the floor and inside the dolly track. An additional camera (iPhone 4; Apple, Cupertino, CA, USA) was installed on the tripod dolly to record the values on the tape measure on the floor. This made it possible to accurately match the photographed image and the distance between the model eye and the target.

During the recording, the dolly was pushed as the researcher walked. The speed was lowered slightly within 1.5 m. The IOLs were held between two lens adapters with a 3.8-mm aperture.

For quantitative analysis, photographs taken at a distance corresponding to each vergence in 0.125 D increments from 0.167 D (6 m) were captured from the videos. For quantitative analysis, 0.118 cycles/mm (1 cycle = 8.5 mm) lines were selected from the resolution target (Fig. 3). This corresponds to 12.3 cycles/degree

at 6 m and 4/20 on the Snellen visual acuity chart. The lines closest to 12.3 cycles/degree in the photos were selected at each distance. Using the ImageJ program, we set a rectangle that crosses the lines, obtained a profile plot (Fig. 5), and measured the resolution (contrast modulation) using the following equation.

$$\text{Contrast modulation} = (\text{Imax} - \text{Imin}) / (\text{Imax} + \text{Imin})$$

The defocus curve was obtained by calculating the contrast modulation at each distance.

Night Street

Headlights, tail lights of cars, and the traffic lights on the street were recorded as a video at night (April 5, 2021, Gukjegeumyung-ro, Yeongdeungpo-gu, Seoul, Korea) to check how streets are perceived by patients with multifocal IOLs at night. The night street was recorded as a video with the mobile model eye installed on the tripod. The aperture size of the IOL adapter was set to 4.8 mm to simulate the situation in which the human pupil becomes dilated at night.

Results

The image of an external object is focused after passing through the artificial cornea and IOL. It is then focused again on the imaging sensor of the DSLR camera after passing through the objective lens and the tube lens. Therefore, the image became upside down, and laterally inverted. For convenience, all photos or videos in the results are rotated 180° from the original photos or videos.

A Distant Building, Daytime (Photograph: 8256 × 5504 Pixels)

The letters on the signboard were clearly visible with monofocal IOLs (Fig. 6A). The edge of the photograph was slightly blurred due to the spherical aberration of the lenses in the mobile model eye. No halo was

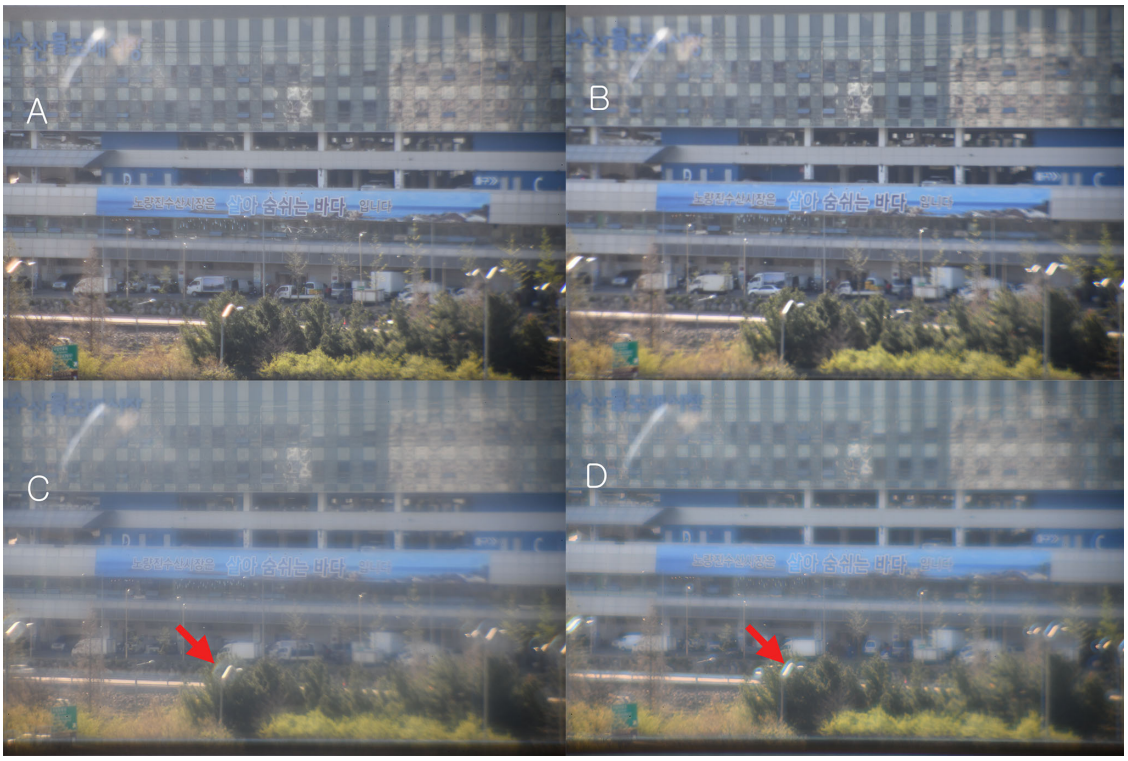

Figure 6. A distant building, daytime. (A) With monofocal IOL, the letters on the signboard were clearly visible. The edge of the photo was slightly blurred due to the spherical aberration of the lenses in the mobile model eye. No halo was observed. In the upper left corner, internal reflection by the windows in the mobile model eye was observed. (B) Eyhance showed a very similar result to monofocal IOL. However, the signboard looked slightly blurry compared to the monofocal IOL. Halo was not rarely observed. (C) With bifocal IOLs, the signboard looked hazy and foggy compared to the monofocal IOLs. The sunlight strongly reflected from the top of the street lamp. A halo (diameter: 360 pixels) was observed around it (*arrow*). (D) Symfony showed a similar result to bifocal IOLs. With Symfony, the signboard looked hazy and foggy compared to monofocal IOLs. A halo (diameter: 157 pixels) was observed around the street lamp (*arrow*). However, it is smaller and considerably stronger than the halo of bifocal IOL.

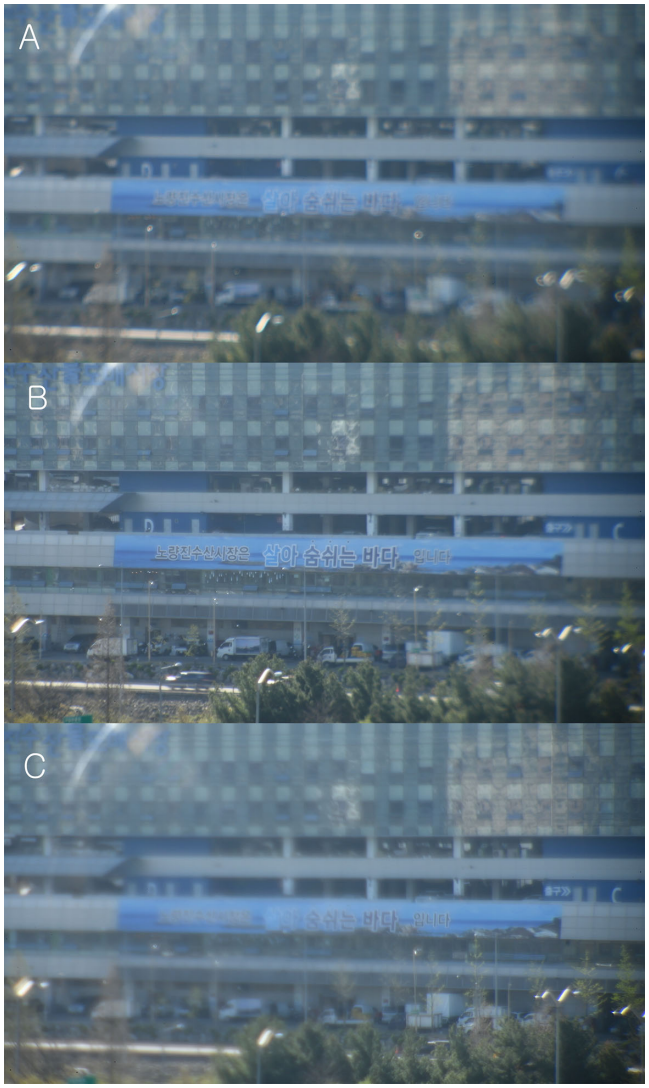

Figure 7. Focusing with monofocal IOL. With monofocal intraocular lens, the letters on the signboard were clearly visible when the focus was on the focal plane of an objective lens. However, they became blurry as the focus passed the focal plane of the objective lens. (A) The focus of the monofocal IOL in front of the focal plane of objective lens. (B) The focus of the monofocal IOL at the focal plane of objective lens. (C) The focus of the monofocal IOL behind the focal plane of objective lens. The focus of the monofocal IOL was 0.44 mm closer to the focal plane of objective lens than panel A.

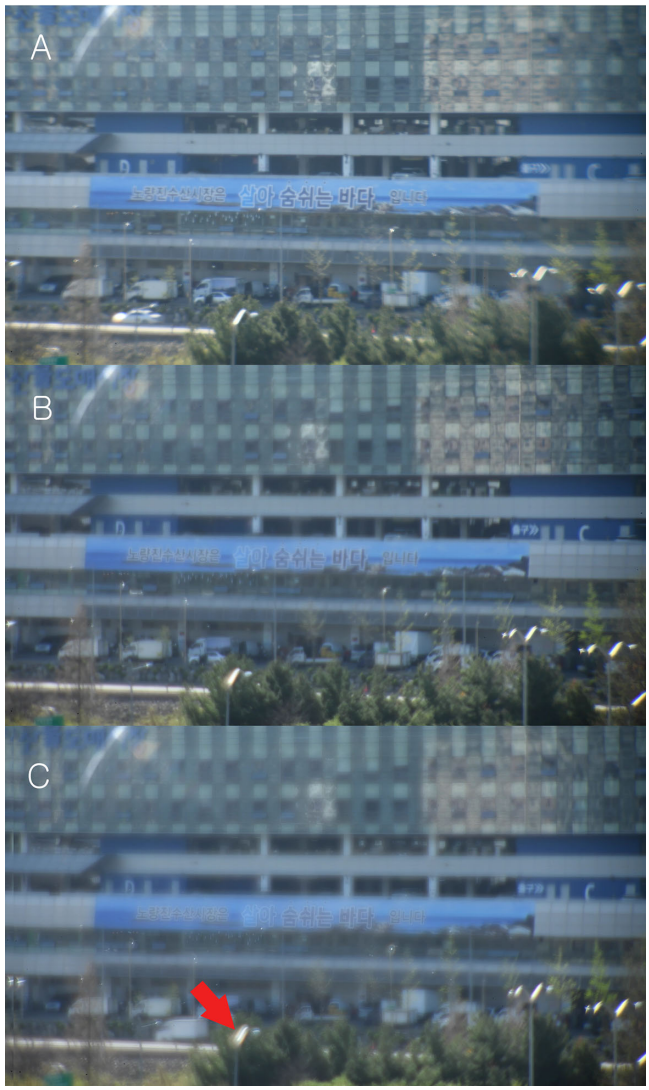

Figure 8. Focusing with Eyhance. (A) With Eyhance, when the far focus was on the focal plane of the objective lens, the image was clear. (B) As the cornea-IOL complex approached the objective lens, the image became slightly blurry. (C) Then, it became slightly clearer again. At this time, a halo was observed around the street lamp, which was small (diameter: 60 pixels) but strong (*arrow*). There was a clear image of street lamp by the second focus of Eyhance inside the halo.

observed. In the upper left corner, internal reflection by the windows in the mobile model eye was observed. Eyhance showed a very similar result to monofocal IOL (Fig. 6B). However, the signboard looked slightly blurry compared to the monofocal IOL. Halo was not observed. With bifocal IOLs, the signboard looked hazy and foggy compared to the monofocal IOLs (Fig. 6C). The sunlight strongly reflected from the top of the street lamp. A halo (diameter: 360 pixels) was observed around it. Symfony showed a similar result to bifocal IOLs. With Symfony, the signboard looked hazy and foggy compared to monofocal IOLs (Fig. 6D). A halo (diameter: 157 pixels) was observed around the street lamp. However, it was smaller and slightly more intense than that of bifocal IOLs.

Focusing (Video: 3840 × 2160 Pixels)

With monofocal IOL, the letters on the signboard were clearly visible when the focus was on the focal plane of an objective lens (Supplementary

Figure 9. Focusing with bifocal IOL. (A) With the bifocal IOL, the image was hazy and foggy compared to the monofocal IOL when the first (far) focus is on the focal plane of the objective lens, and the halo (diameter: 171 pixels) is observed around the street lamp (*arrow*). (B) As the cornea-IOL complex approached the focal plane of the objective lens, the image became significantly blurry. (C) Then, it became clear again when the second (near) focus was on the objective lens. At this time, the halo (diameter: 203 pixels) was observed around the street lamp (*arrow*).

Movie S1, Fig. 7). However, they became blurry as the focus passed the focal plane of the objective lens.

With Eyhance, when the far focus was on the focal plane of the objective lens, the image was clear (Supplementary Movie S2, Fig. 8). As the cornea-IOL complex approached the objective lens, the image became slightly blurry, followed by becoming slightly clearer again. At this time, a halo was observed around the street lamp, which was small (diameter: 60 pixels) but strong. Afterward, the image became blurry again. With bifocal IOLs, the image was hazy and foggy compared to the monofocal IOL when the first (far)

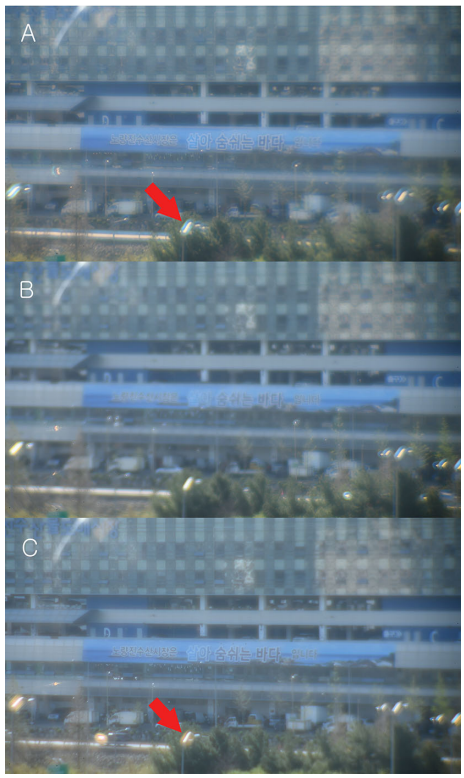

Figure 10. Focusing with Symfony. (A) With Symfony, the image is hazy and foggy compared to that with the monofocal IOL. The halo (diameter: 81 pixels) was observed around the street lamp (*arrow*). (B) As the cornea-IOL complex approached the focal plane of the objective lens, the image became blurry. (C) Then, it became clear again when the second (near) focus was on the objective lens. The halo (diameter: 85 pixels) around the street lamp (*arrow*) at the second focus was slightly weaker than that at the first focus. The two foci were significantly closer compared to the foci in the bifocal IOL. The images were not very blurry in this interval compared to the bifocal IOL.

focus is on the focal plane of the objective lens, and the halo (diameter: 171 pixels) is observed around the street lamp (Supplementary Movie S3, Fig. 9). As the cornea-IOL complex approached the focal plane of the objective lens, the image became significantly blurry, then clear again when the second (near) focus was on the objective lens. At this time, a halo (diameter: 203 pixels) was observed around the street lamp. However, the intensity was slightly weaker than that of the halo in the first focus. Afterward, the image became blurry again.

With Symfony, the image is hazy and foggy compared to that with the monofocal IOL (Supplementary Movie S4, Fig. 10). The image was taken when the first (far) focus was on the focal plane of the objective lens. The halo (diameter: 81 pixels) was observed around the street lamp. As the cornea-IOL complex approached the objective lens, the image became blurry and then clear again. The image was taken when the second focus was on the focal plane of

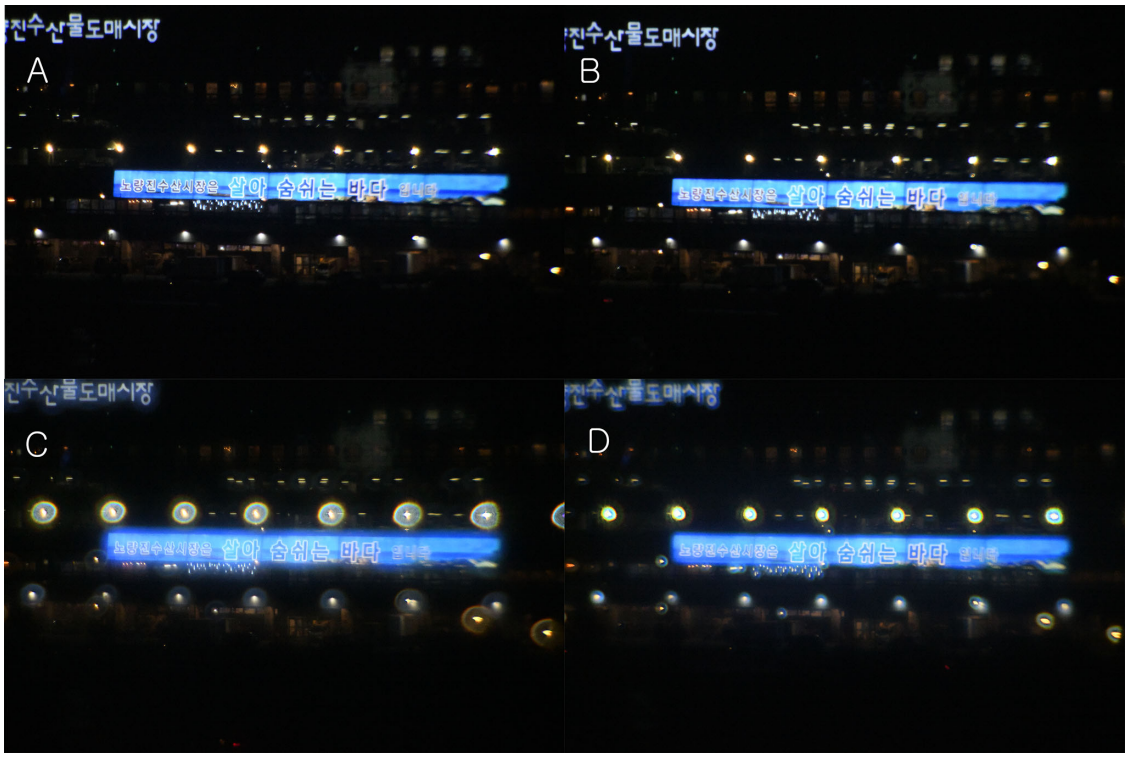

Figure 11. A distant building, night. (A) The signboard looks relatively clear with monofocal IOL. Halo was not observed around the lights above and below the signboard. (B) It was slightly more blurred with Eyhance than the monofocal IOL. No halo was observed. (C) With the bifocal IOL, the letters on the signboard were blurred as compared to the monofocal IOL. A circular halo is clearly visible around the lights above and below the signboard. (D) In Symfony, the letters on the signboard were blurred as compared to the monofocal IOL. It is similar to the bifocal IOL. The size of the halo (234 pixels) around the lights above and below the signboard is smaller than that of the bifocal IOL (432 pixels).

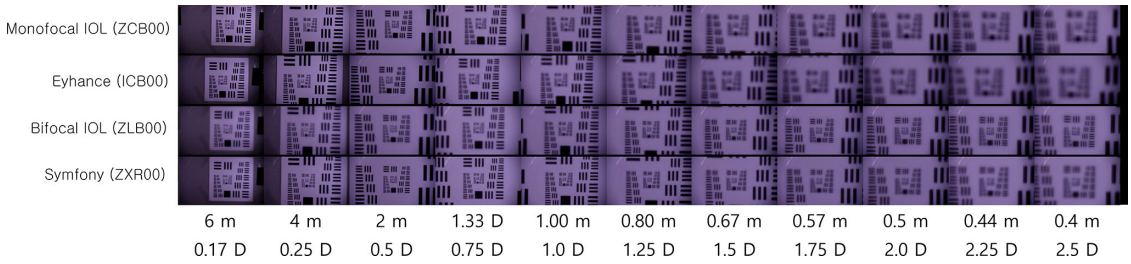

Figure 12. A 6 m distance USAF 1951 resolution target. (A) With the monofocal IOL, the image was significantly clear at 6 m. However, it blurred as the model eye approached the resolution target. (B) With Eyhance, the image appeared slightly more blurred than the monofocal IOLs at 6 m. As it approached the resolution target, it blurred. However, at 80 to 155 cm, the image looked clearer than that by the monofocal IOL. (C) With the bifocal IOL, the image was hazy compared to that with the monofocal IOL at 6 m. As it got closer, it blurred considerably. Then, it became clear again at approximately 50 to 60 cm. After that, the clarity decreased as the distance decreased. (C) With Symfony, the image was hazier compared to that with the monofocal IOL at 6 m. As the distance between them decreased, the image blurred. Then, it became clear again at approximately 90 to 110 cm. After that, the clarity decreased as the distance decreased.

the objective lens. The two foci were significantly closer compared with the foci in the bifocal IOL. The images obtained using Symfony were not very blurry at this interval compared with that of the bifocal IOL. The signboard looks slightly clearer at the second (intermediate distance) focus than at the first (far) focus. The halo (diameter: 85 pixels) around the street lamp at the second focus was slightly weaker than that at the first focus.

A Distant Building, Night (Photograph: 8256 × 5504 Pixels)

The signboard looks relatively clear with monofocal IOLs (Fig. 11A). Halo was not observed around the lights above and below the signboard. It was slightly more blurred with Eyhance than that with monofocal IOLs (Fig. 11B). No halo was observed. With the bifocal IOL, the letters on the signboard were blurred

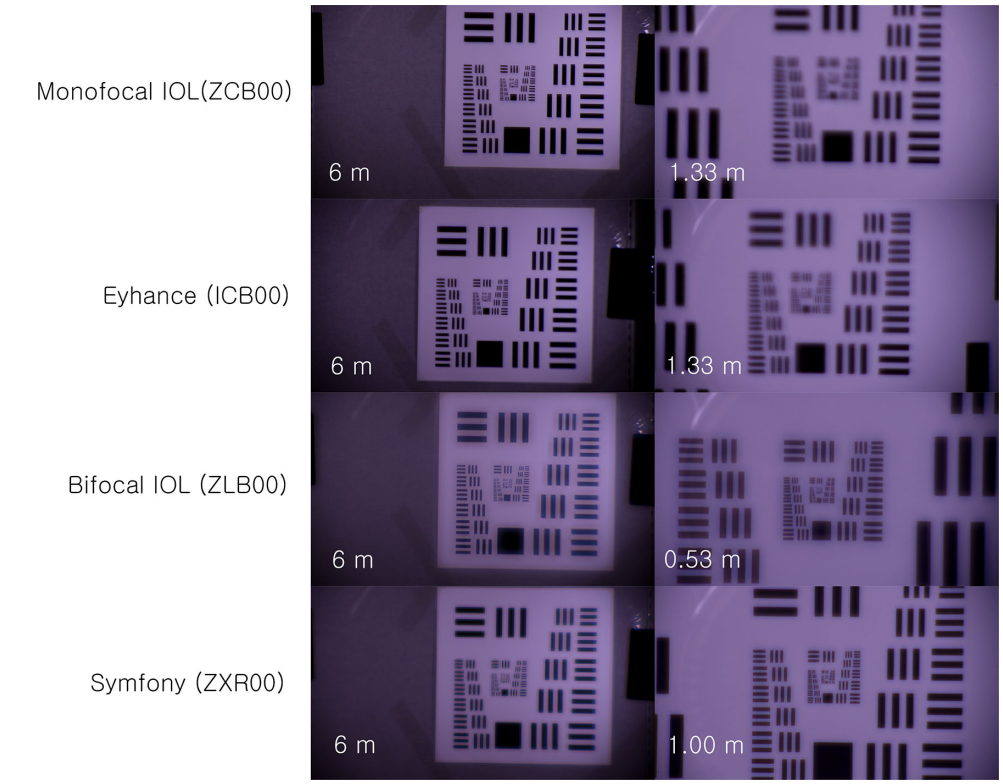

Figure 13. The resolution target images at 6 m and near or intermediate distances with four intraocular lenses. (A) With the monofocal IOL, the image was significantly clear at 6 m. However, it blurred as the model eye approached the resolution target. (B) With Eyhance, the image appeared slightly more blurred than the monofocal IOLs at 6 m. There was no ghost image around the lines. As it approached the resolution target, it blurred. However, at 80 to 155 cm, the image looked clearer than that by the monofocal IOL. At this time, ghost images (background images) were observed at the edge of the lines. (C) With the bifocal IOL, the image was hazy compared to that with the monofocal IOL at 6 m. Ghost images were visible around the lines. As it got closer, it blurred considerably. Then, it became clear again at approximately 50 to 60 cm. At this time, the ghost images were observed around the lines. These were weaker than the ghost images at 6 m. (D) With Symfony, the image was hazier compared to that with the monofocal IOL at 6 m. Ghost images were observed around the lines. However, they were narrower than that of bifocal IOL. As the distance between them decreased, the image blurred. Then, it became clear again at approximately 90 to 110 cm. At this time, ghost images were observed around the lines. However, they were narrower than the ghost images at near focus (approximately 50–60 cm) with the bifocal IOL. These ghost images were less intense than the ghost images at 6 m.

compared with the monofocal IOL (Fig. 11C). A circular halo is clearly visible around the lights above and below the signboard in Figure 11C. In Symfony, the letters on the signboard were blurred as compared with the monofocal IOL (Fig. 11D). It is similar to the bifocal IOL. The size of the halo (diameter: 234 pixels) around the lights above and below the signboard is smaller than that of the bifocal IOL (diameter: 432 pixels).

A 6 m Distance USAF 1951 Resolution Target (Video: 3840 × 2160 Pixels)

Supplementary Movies S5 to S8 were recorded continuously when the mobile model eye approached the USAF 1951 resolution target from 6 m to 15 cm. The viewing angle was 9.3° horizontally and 5.3° vertically. The rail joint rattled and the dolly moved left and right as it approached the resolution target.

With the monofocal IOL, the image was significantly clear at 6 m (Supplementary Movie S5, Figs. 12, 13). However, it blurred as the model eye approached the resolution target. With Eyhance, the image appeared slightly more blurred than that with the monofocal IOLs at 6 m (Supplementary Movie S6, Figs. 12, 13). There was no ghost image around the lines. Blurring was observed as the model eye approached the resolution target. However, at 80–155 cm, the image looked clearer than that with the monofocal IOL and ghost images (background images) were observed at the edge of the lines. With the bifocal IOL, the image was hazy compared with that of the monofocal IOL at 6 m (Supplementary Movie S7, Figs. 12, 13). Ghost images were visible around the lines. Blurring was observed as the model eye got closer

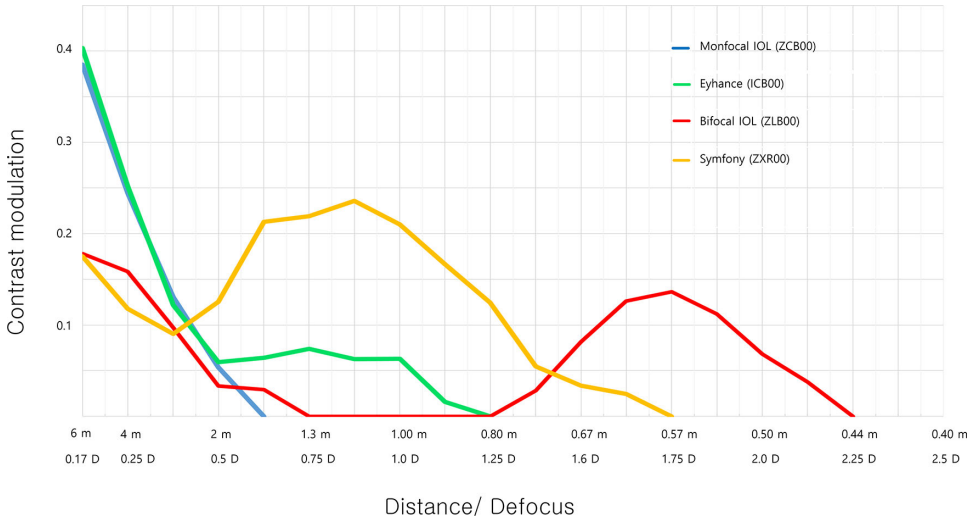

Figure 14. Defocus curves of monofocal IOL, Eyhance, bifocal IOL and Symfony. For monofocal IOL, the contrast modulation was 0.39 at 6 m (0.167 D) and decreased consistently. It was nearly 0 from 1.6 m (0.625 D). For Eyhance, the contrast modulation was 0.40 at 6 m. It then decreased and increased again. At 1.3 m (0.75 D), it was 0.07 and then decreased again. For the bifocal IOL, the contrast modulation was 0.18 at 6 m. It is lower than that of monofocal IOL at 6 meters. After that, it decreased to nearly 0 at 80 to 130 cm. It increased again to 0.14 at 57 cm (1.75 D) and then decreased again. For Symfony, the contrast modulation was 0.18 at 6 m. It is lower than that of the monofocal IOL at 6 m. After that, it decreased and increased to 0.24 at 114 cm (0.875 D) and then decreased again.

and the image became clear again at approximately 50 to 60 cm. Ghost images were observed around the lines at this time, which were less intense than the ghost images at 6 m. Subsequently, the clarity decreased as the distance decreased. With Symfony, the image was hazier compared to that with the monofocal IOL at 6 m (Supplementary Movie S8, Figs. 12, 13). Ghost images were observed around the lines. However, they were narrower than that of bifocal IOL. As the distance between them decreased, the image was blurred and

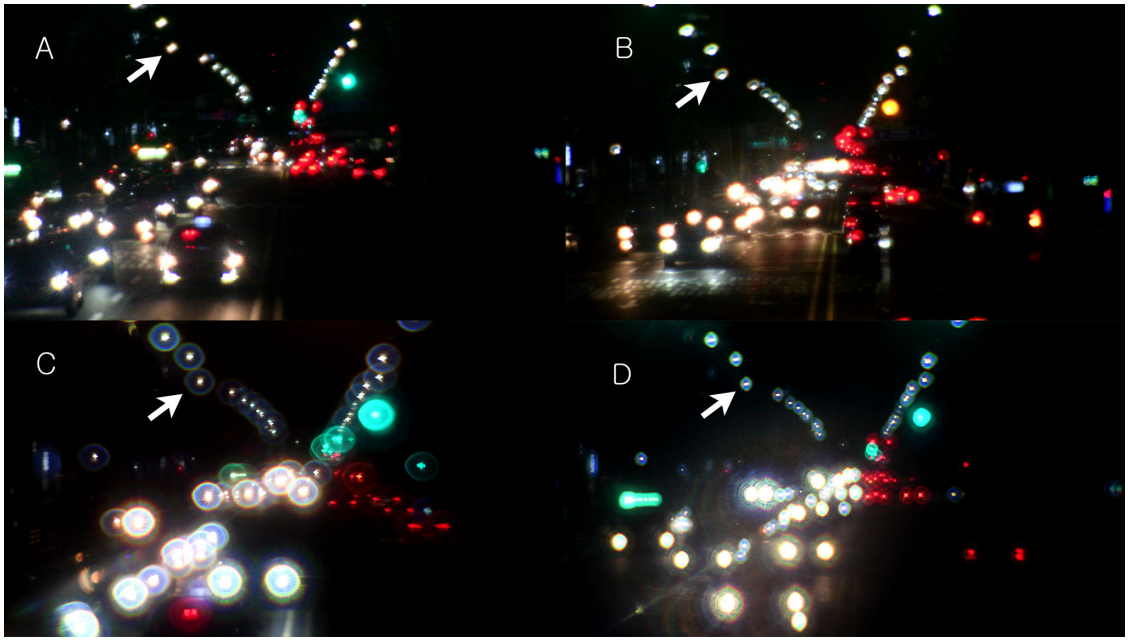

Figure 15. Night street. (A) With the monofocal IOL, the pixels looked rough compared to the daytime. However, there was no definite halo around the headlights, tail lights of the cars, and traffic lights. (B) Eyhance is similar to the monofocal IOL. However, there are few small halos (75 pixels) (*arrow*) around street lamps compared to monofocal IOL. (C) In the image with the bifocal IOL, the halo around the headlights, tail lights of the cars, traffic lights, and street lamps (185 pixels) (*arrow*) were definite and large compared to the monofocal IOL. (D) Symfony is similar to the bifocal IOL. However, the size of the halo (street lamp: 85 pixels) (*arrow*) was smaller than that of the bifocal IOL.

then became clear again at approximately 90 to 110 cm. Ghost images were observed around the lines at this time. However, they were narrower than the ghost images at near focus (approximately 50–60 cm) with the bifocal IOL. These ghost images were less intense than the ghost images at 6 m. The clarity decreased subsequently as the distance decreased. Figure 13 shows the resolution target images at 6 m and near or intermediate distances with four IOLs.

Figure 14 shows the defocus curve obtained by calculating the contrast modulation of the above resolution target images. For monofocal IOL, the contrast modulation was 0.39 at 6 m (0.167 D) and decreased consistently. It was nearly 0 as the model eye got closer than 1.6 m (0.625 D). For Eyhance, the contrast modulation was 0.40 at 6 m. It then decreased and increased again. At 1.3 m (0.75 D), it was 0.07 and then decreased again. For the bifocal IOL, the contrast modulation was 0.18 at 6 m, which is lower than that of monofocal IOL at 6 m. Subsequently, it decreased to nearly 0 at 80 to 130 cm. It increased again to 0.14 at 57 cm (1.75 D) and then decreased again. For Symfony, the contrast modulation was 0.18 at 6 m, which is lower than that of the monofocal IOL at 6 m. It subsequently decreased and increased to 0.24 at 114 cm (0.875 D) and then decreased again.

Night Street (Video: 3840 × 2160 Pixels)

Figure 15 shows the results of the night street measurement. With the monofocal IOL, the pixels at night time looked rough compared with that at the daytime (Supplementary Movie S9). However, there was no definite halo around the headlights, tail lights of the cars, and traffic lights. Eyhance is similar to monofocal IOL (Supplementary Movie S10). However, there were a few small halos (diameter: 75 pixels) around the street lamps compared with monofocal IOL (diameter: 52 pixels). In the image obtained with bifocal IOL, the halo around the headlights, tail lights of the cars, traffic lights, and street lamps (diameter: 185 pixels) were definite and large compared with the monofocal IOL (Supplementary Movie S11). Symfony is similar to bifocal IOL. However, the size of the halo (street lamp: 85 pixels) was smaller than that of the bifocal IOL (Supplementary Movie S12).

Discussion

In this revised model eye using an objective lens, an artificial cornea similar to the human cornea can be used. Using a DSLR camera, high-resolution imaging was possible without an additional computer. Fine focusing was possible using an adjustable lens tube. The results of testing with this revised model eye suggest that Eyhance had slightly better optical quality (contrast modulation: 0.07) at an intermediate distance than the monofocal IOL (contrast modulation: nearly zero). It had slightly inferior far distance optical quality and showed a slight halo at night. Symfony showed the characteristics of a bifocal IOL with low add power. Far objects looked hazy and foggy compared to monofocal IOL. Halo around lights was observed. However, their size (234 pixels) was smaller than that of the bifocal IOL (432 pixels).

This experimental study had two purposes: to check the performance of the revised model eye, which is an improvement on our previous mobile model eye[1] and to check how the world is perceived by patients with monofocal IOL, Eyhance, bifocal IOL, and Symfony using this revised model eye and compare them.

This revised mobile model eye has some advantages over our previous mobile model eye. First, our revised model eye used an objective lens. Hence, the flange distance (46.50 mm) of the DSLR camera did not restrict the focal length of the artificial cornea and the IOL base power. The focal length of the artificial cornea lens can be selected as a value similar to that of the human cornea. The IOL base power could be freely selected. Second, we used a DSLR camera instead of a complementary metal–oxide–semiconductor scientific camera in our previous study. Thus the resolution was significantly higher than that of the complementary metal–oxide–semiconductor camera. Additionally, it was convenient to use as a mobile device because an additional computer was not needed. Third, we used an adjustable lens tube in the revised model eye. In our previous study, we had to slide the cornea-IOL complex within the cage for focusing. Hence, fine focusing was difficult. In this revised mobile model eye, significantly more sophisticated focusing was achieved. Using this adjustable lens tube, the focusing process was recorded continuously as a video. Thus, the multifocal function was intuitively proven. Fourth, a dolly track was used for shooting the movie. The mobile model eye approached the USAF 1951 target from 6 m to 15 cm. The image was continuously recorded as a video. Therefore, the multifocal function was intuitively proven again. A defocus curve was obtained by calculating the contrast modulation of the above-mentioned resolution images. This test format of taking photographs of distant buildings during the day and at night, video recording of the focusing process, video recording of USAF resolution target from 6 m to 15 cm, quantitative analysis, and taking a photograph of night street will be used for

evaluating other multifocal IOLs in our subsequent studies.

However, this revised mobile model eye still has some limitations. First, we required a tube lens because we used an objective lens. Therefore the model eye became larger and heavier than the previous model. In addition, using a DSLR camera instead of a scientific camera made an additional computer unnecessary. However, the mobile model eye itself became heavier. Since we used an objective lens, the image became upside down, and laterally inverted. There was no problem in recording the video of the model's eye moving on the dolly track. However, it was inconvenient to record a video when a researcher held it by hand and walked. Complex optical design increases the weight of the model eye and risk of errors in focusing and alignment. We are developing another mobile model eye in which images are focused at the sensor of DSLR camera directly without objective lens. Second, the near focus of the bifocal IOL was slightly different from the provided in the company data. According to the data (https://www.jnjvisionpro.com/products/tecnis%C2%AE-multifocal-iol-325-d) provided by J&J, the additional power in the spectacle plane of the bifocal IOL (add 3.25 D, ZLB00) is 2.37 D. Thus theoretically, the object at 42 cm from the artificial cornea should be clearly visible by the additional power. However, the object at 57 cm from the artificial cornea was clearly visible in our experiments. This is due to the large distance between the artificial cornea and IOL. In this model eye, we decreased the distance between the artificial cornea and the IOL as much as possible. However, it was still significantly larger than that in the human eye. In this experiment, the distance between the posterior surface of the artificial cornea and the center of the IOL was 6.8 mm. Because the central thickness of the artificial cornea was 5.35 mm, the distance between the anterior cornea and the center of the IOL was 12.15 mm. Contrarily, in the human eye, the average central corneal thickness is 0.5 mm,[50] the anterior chamber depth is 3.2 mm,[50] and the lens thickness is 4.0 mm.[51] Therefore the distance between the anterior surface of the cornea and the center of the lens is 5.7 mm, which is significantly different. Because of this difference, the object at 57 cm from the artificial cornea was clearly visible in our experiments instead of 42 cm. This experiment discovered the overall trend of the clarity of the resolution target at far, intermediate, and near distances through the bifocal IOL. The exact value of 42 cm or 57 cm is not crucial for this experiment.

Third, the approaching speed in the dolly track was not constant, as the researcher walked and pushed the dolly loaded with the revised model eye. However, it did not affect the quantitative analysis of the defocus curve. Currently, we are attempting to motorize this system. The rail joint rattled and the dolly moved left and right as it approached the resolution target. This issue was caused due to the multiple connected track segments. This limitation can be resolved by using a track with solid seams.

In this study, the pupil size was 3.8 mm in the daytime or indoor photography and 4.8 mm at night considering the dilatation of the human pupil. Even at an identical distance and lighting, if the pupil (aperture) size is changed, the result may be different. In the subsequent study, we will experimentally vary the diameter of the pupil by installing an easily changeable aperture. In addition, this experiment was conducted under natural or white (polychromatic) light. In the optical bench tests, experiments are often performed only at a single wavelength (approximately 530 nm)[42,43,45,46] to eliminate chromatic aberration. Experimenting in natural or white light will provide more realistic results. Lee et al.[44] measured the defocus curve of Symfony using the polychromic light similar to our experiment and showed a defocus curve similar to our results.

We investigated how the world is perceived by patients with monofocal IOL, Eyhance, bifocal IOL, and Symfony using this revised model eye and compared the results. Eyhance showed similar results to monofocal IOLs at a far distance. However, with Eyhance the USAF resolution target was slightly clearer (contrast modulation: 0.07) at intermediate distances compared with the monofocal IOL (contrast modulation: nearly zero). There were a few small halos in the night street recording. With Symfony, the objects that were far (contrast modulation: 0.18) looked hazy and foggy compared with the monofocal IOLs (contrast modulation: 0.39). However, objects at an intermediate distance looked relatively clearer (contrast modulation: 0.24) compared with the monofocal IOL (contrast modulation: nearly zero). Symfony functions similar to a bifocal lens with low add power. Halos (234 pixels) were observed with sizes smaller than those with the bifocal IOL (432 pixels).

The literature on the Eyhance showed no difference in distance visual acuity compared with monofocal IOL in clinical studies.[4–6,52] Eyhance had better intermediate distance visual acuity than monofocal IOLs.[4–6,52] No halo was observed.[6] In our study, unlike the earlier studies, the optical quality of far objects was slightly lower than that of monofocal IOLs. A halo with reduced intensity was observed in the night street recording. The defocus curve of Eyhance shown in the clinical study[4–7] was similar to our results. An experimental study measured Eyhance's defocus curve

in the optical bench test.[8] The defocus curve was similar to ours. However, photographs of a USAF1951 resolution target on an optical bench were taken in that study. They did not show how the real world appears to patients with Eyhance. According to clinical studies on Symfony, the base of the defocus curve of Symfony broadened at 0 D compared with monofocal IOL.[9–41] However, some experimental studies[42–46] showed the defocus curves of bifocal IOL with low add power similar to our study. In other clinical studies, the halos with Symfony were observed in 2% to 95% of cases.[3,9,13,19,21,27,30,31,35,36,40,47–49] Although the halo was observed herein, the size was smaller than that of bifocal IOLs.

The defocus curve (Fig. 14) was obtained by quantitatively analyzing the video taken while the mobile model eye approached the resolution target from 6 m to 15 cm. With the defocus curve obtained in this way, the light energy distribution of the lens could be estimated. Eyhance had contrast modulations of 0.40 and 0.07 at a far distance (6 m) and an intermediate distance (1.3 m), respectively. Therefore most of the light energy was focused on the far focus. Only a part of the light was focused on the intermediate distance focus. The bifocal IOL had a contrast modulation of 0.18 at a far distance (6 m). The contrast modulation decreased at an intermediate distance and increased again to 0.14 at 57 cm. This is similar to the contrast modulation at a far distance. Therefore, similar light energy was focused at far and near focus. According to data provided by the company, the light distribution between the distance and near focus was approximately 50/50 (accessdata.fda.gov/cdrh_docs/pdf/p980040s049d.pdf). The contrast modulation at a far distance of Symfony was similar to that of the bifocal IOL (contrast 0.18). It then decreased and increased again. At the intermediate distance (near 114 cm), the contrast modulation showed the highest value of 0.24. Therefore the light distribution at an intermediate distance was slightly higher than at a far distance. However, according to the results of the previous experimental studies[42–46] on Symfony, the light distribution at the far and intermediate distances was generally similar.

The intensity and size of the halo or ghost image, which are unavoidable disadvantages of multifocal IOLs, can be predicted from the defocus curve of the lens. The intensity of halo can be explained by the light energy distribution. It can be estimated by the defocus curve. If a greater amount of light energy goes to the far focus than to the near focus, the halo will be stronger at the near distance. However, it will be weaker at a far distance. Conversely, if a greater amount of light energy goes to the near focus than the far focus, the halo will be weaker at the near distance, and stronger at the far distance. In our experiment on Eyhance, a greater amount of light energy went to the far focus than the intermediate focus. The halo at the second focus (intermediate distance) was stronger than the halo at the first focus (far distance) (Supplementary Movie S2, Fig. 8). Conversely, in Symfony, slightly greater amount of light energy went to the intermediate focus than the far focus. The halo in the second focusing (intermediate distance) had weaker intensity than the halo in the first focusing (far distance) (Supplementary Movie S4, Fig. 10).

The size of the halo can be explained by the diopter difference between the two foci in the defocus curve. In the bifocal lens with a large diopter difference between the two foci, the halo is large at far (Fig. 9A [street lamp: 171 pixels], 15C [street lamp: 185 pixels]) and near distances (Fig. 9C) (street lamp: 203 pixels). In Eyhance and Symfony with a smaller diopter difference between the two foci, the halo is small in the far (Figs. 8A, 10A [street lamp: 81 pixels], 15B [street lamp: 75 pixels], 15D [street lamp: 85 pixels]) and intermediate distances (Fig. 8C [street lamp: 60 pixels], 10C [street lamp: 85 pixels]). These halos were observed significantly more clearly at night (Figs. 11, 15) than during the day. Ghost images also showed a tendency (Fig. 13) similar to the halos.

If a multifocal IOL is not an accommodative IOL, it is theoretically impossible to have a multifocal function without halo and a decreased distant visual acuity. For better visual acuity at an intermediate or near distance compared to monofocal IOL, the visual acuity at far distance should decrease. A halo or ghost image is generated inevitably. The size and intensity of the halo can vary depending on the added power and light energy distribution of the IOLs.

Decreased optical quality for far objects, halo, and ghost images of the multifocal IOL shown in this experiment may differ from those actually perceived by the patients due to the neural adaptation[53] of their brains. To overcome these shortcomings, we developed a see-through IOL simulator that allows patients to directly perceive the world through the IOLs. It allows the patient to directly experience far, near, and halo through monofocal IOL and multifocal IOL.[54] As a result, similar to this study, the visual acuity with bifocal IOL at a near distance is better,[54] whereas it is worse at a far distance. More halos were perceived by the patients compared with monofocal IOL.

In conclusion, we could objectively observe and compare how patients with monofocal IOL, Eyhance, bifocal IOL, and Symfony perceived the world using this revised model eye. In this revised model eye using an objective lens, an artificial cornea similar to the human cornea can be used. Using a DSLR camera, high-resolution imaging was possible without

an additional computer. Fine focusing was possible using an adjustable lens tube. This test format of taking photographs of distant buildings during the day and at night, video recording of the focusing process, video recording of USAF resolution target from 6 m to 15 cm, quantitative analysis, and taking a photograph of night street will be used for evaluating other multifocal IOLs in our subsequent studies.

Acknowledgments

Supported by a grant from the Korea Health Technology R&D Project through the Korea Health Industry Development Institute (KHIDI), funded by the Ministry of Health & Welfare, Republic of Korea (grant number: HI17C0659), Basic Science Research Program through the National Research Foundation of Korea (NRF), funded by the Ministry of Education, Republic of Korea (No. 2017R1A1A2A10000681, 2020R1A2C1005009, 2022R1F1A1069218).

The Catholic University of Korea (inventor: Ho Sik Hwang) has issued a Korea patent (10-2132214) for the revised mobile model eye tested in the study.

Disclosure: **E.C. Kim,** None; **S.Y. Cho,** None; **J.E. Kang,** None; **G. Nam,** None; **Y.C. Yoon,** None; **W.-J. Whang,** None; **K.-S. Na,** None; **H.-S. Kim,** None; **H.S. Hwang,** None

References

1. Kim EC, Na KS, Kim HS, Hwang HS. How does the world appear to patients with multifocal intraocular lenses?: a mobile model eye experiment. *BMC Ophthalmol*. 2020;20:180.
2. Sridhar MS. Anatomy of cornea and ocular surface. *Indian J Ophthalmol*. 2018;66:190–194.
3. Cochener B, Concerto Study Group. Clinical outcomes of a new extended range of vision intraocular lens: International Multicenter Concerto Study. *J Cataract Refract Surg*. 2016;42:1268–1275.
4. Mencucci R, Cennamo M, Venturi D, Vignapiano R, Favuzza E. Visual outcome, optical quality, and patient satisfaction with a new monofocal IOL, enhanced for intermediate vision: preliminary results. *J Cataract Refract Surg*. 2020;46:378–387.
5. Yangzes S, Kamble N, Grewal S, Grewal SPS. Comparison of an aspheric monofocal intraocular lens with the new generation monofocal lens using defocus curve. *Indian J Ophthalmol*. 2020;68:3025–3029.
6. Kang KH, Song MY, Kim KY, Hwang KY, Kwon YA, Koh K. Visual performance and optical quality after implantation of a new generation monofocal intraocular lens. *Korean J Ophthalmol*. 2021;35:112–119.
7. Auffarth GU, Gerl M, Tsai L, et al. Clinical evaluation of a new monofocal IOL with enhanced intermediate function in patients with cataract. *J Cataract Refract Surg*. 2021;47:184–191.
8. Huh J, Eom Y, Yang SK, Choi Y, Kim HM, Song JS. A comparison of clinical outcomes and optical performance between monofocal and new monofocal with enhanced intermediate function intraocular lenses: a case-control study. *BMC Ophthalmol*. 2021;21:365.
9. Monaco G, Gari M, Di Censo F, Poscia A, Ruggi G, Scialdone A. Visual performance after bilateral implantation of 2 new presbyopia-correcting intraocular lenses: trifocal versus extended range of vision. *J Cataract Refract Surg*. 2017;43:737–747.
10. Pedrotti E, Carones F, Aiello F, et al. Comparative analysis of visual outcomes with 4 intraocular lenses: monofocal, multifocal, and extended range of vision. *J Cataract Refract Surg*. 2018;44:156–167.
11. Cochener B, Boutillier G, Lamard M, Auberger-Zagnoli C. A comparative evaluation of a new generation of diffractive trifocal and extended depth of focus intraocular lenses. *J Refract Surg*. 2018;34:507–514.
12. Farvardin M, Johari M, Attarzade A, Rahat F, Farvardin R, Farvardin Z. Comparison between bilateral implantation of a trifocal intraocular lens (Alcon Acrysof IQ PanOptix) and extended depth of focus lens (Tecnis Symfony ZXR00 lens). *Int Ophthalmol*. 2021;41:567–573.
13. Schallhorn JM. Multifocal and extended depth of focus intraocular lenses: a comparison of data from the United States Food and Drug Administration premarket approval trials. *J Refract Surg*. 2021;37:98–104.
14. Liu X, Song X, Wang W, et al. Comparison of the clinical outcomes between echelette extended range of vision and diffractive bifocal intraocular lenses. *J Ophthalmol*. 2019;2019:5815040.
15. Escandón-García S, Ribeiro FJ, McAlinden C, Queirós A, González-Méijome JM. Through-focus vision performance and light disturbances of 3 new intraocular lenses for presbyopia correction. *J Ophthalmol*. 2018;2018:6165493.

16. Ganesh S, Brar S, Pawar A, Relekar KJ. Visual and refractive outcomes following bilateral implantation of extended range of vision intraocular lens with micromonovision. *J Ophthalmol*. 2018;2018:7321794.
17. Lee JH, Chung HS, Moon SY, et al. Clinical outcomes after mix-and-match implantation of extended depth of focus and diffractive multifocal intraocular lenses. *J Ophthalmol*. 2021;2021:8881794.
18. Pilger D, Homburg D, Brockmann T, Torun N, Bertelmann E, von Sonnleithner C. Clinical outcome and higher order aberrations after bilateral implantation of an extended depth of focus intraocular lens. *Eur J Ophthalmol*. 2018;28:425–432.
19. Lee JH, Moon SY, Chung HS, et al. Clinical outcomes of a monofocal intraocular lens with enhanced intermediate function compared with an extended depth-of-focus intraocular lens. *J Cataract Refract Surg*. 2022;48:61–66.
20. Pedrotti E, Bruni E, Bonacci E, Badalamenti R, Mastropasqua R, Marchini G. Comparative analysis of the clinical outcomes with a monofocal and an extended range of vision intraocular lens. *J Refract Surg*. 2016;32:436–442.
21. Webers VSC, Bauer NJC, Saelens IEY, et al. Comparison of the intermediate distance of a trifocal IOL with an extended depth-of-focus IOL: results of a prospective randomized trial. *J Cataract Refract Surg*. 2020;46:193–203.
22. Pedrotti E, Carones F, Talli P, et al. Comparative analysis of objective and subjective outcomes of two different intraocular lenses: trifocal and extended range of vision. *BMJ Open Ophthalmol*. 2020;5(1):e000497.
23. Ruiz-Mesa R, Abengózar-Vela A, Ruiz-Santos M. A comparative study of the visual outcomes between a new trifocal and an extended depth of focus intraocular lens. *Eur J Ophthalmol*. 2018;28:182–187.
24. Gil MA, Varón C, Cardona G, Buil JA. Visual acuity and defocus curves with six multifocal intraocular lenses. *Int Ophthalmol*. 2020;40:393–401.
25. Doroodgar F, Niazi F, Sanginabadi A, et al. Visual performance of four types of diffractive multifocal intraocular lenses and a review of articles. *Int J Ophthalmol*. 2021;14:356–365.
26. Lubiński W, Podborączyńska-Jodko K, Kirkiewicz M, Mularczyk M, Post M. Comparison of visual outcomes after implantation of AtLisa tri 839 MP and Symfony intraocular lenses. *Int Ophthalmol*. 2020;40:2553–2562.
27. Ang RE, Picache GCS, Rivera MCR, Lopez LRL, Cruz EM. A comparative evaluation of visual, refractive, and patient-reported outcomes of three extended depth of focus (EDOF) intraocular lenses. *Clin Ophthalmol*. 2020;14:2339–2351.
28. de Medeiros AL, Jones Saraiva F, Iguma CI, et al. Comparison of visual outcomes after bilateral implantation of two intraocular lenses with distinct diffractive optics. *Clin Ophthalmol*. 2019;13:1657–1663.
29. Palomino-Bautista C, Sánchez-Jean R, Carmona-González D, Piñero DP, Molina-Martín A. Subjective and objective depth of field measures in pseudophakic eyes: comparison between extended depth of focus, trifocal and bifocal intraocular lenses. *Int Ophthalmol*. 2020;40:351–359.
30. Reinhard T, Maier P, Böhringer D, et al. Comparison of two extended depth of focus intraocular lenses with a monofocal lens: a multi-centre randomised trial. *Graefes Arch Clin Exp Ophthalmol*. 2021;259:431–442.
31. Rementería-Capelo LA, García-Pérez JL, Gros-Otero J, Carrillo V, Pérez-Lanzac J, Contreras I. Real-world evaluation of visual results and patient satisfaction for extended range of focus intraocular lenses compared to trifocal lenses. *Int Ophthalmol*. 2021;41:163–172.
32. Son HS, Kim SH, Auffarth GU, Choi CY. Prospective comparative study of tolerance to refractive errors after implantation of extended depth of focus and monofocal intraocular lenses with identical aspheric platform in Korean population. *BMC Ophthalmol*. 2019;19(1):187.
33. Paik DW, Park JS, Yang CM, Lim DH, Chung TY. Comparing the visual outcome, visual quality, and satisfaction among three types of multi-focal intraocular lenses [published correction appears in Sci Rep. 2021 May 3;11(1):9776]. *Sci Rep*. 2020;10(1):14832.
34. Palomino-Bautista C, Sánchez-Jean R, Carmona-Gonzalez D, Piñero DP, Molina-Martín A. Depth of field measures in pseudophakic eyes implanted with different type of presbyopia-correcting IOLS. *Sci Rep*. 2021;11(1):12081.
35. Song X, Liu X, Wang W, et al. Visual outcome and optical quality after implantation of zonal refractive multifocal and extended-range-of-vision IOLs: a prospective comparison. *J Cataract Refract Surg*. 2020;46:540–548.
36. Chang DH, Janakiraman DP, Smith PJ, et al. Visual outcomes and safety of the TECNIS Symfony intraocular lens: results of a pivotal clinical trial. *J Cataract Refract Surg*. 2022;48:288–297.

37. Koo OS, Kang JW, Park JK, Kim KS. Visual performance and patient satisfaction after implantation of extended range-of-vision IOLs: bilateral implantation vs 2 different mix-and-match approaches. *J Cataract Refract Surg*. 2021;47:192–197.
38. Schojai M, Schultz T, Jerke C, Böcker J, Dick HB. Visual performance comparison of 2 extended depth-of-focus intraocular lenses. *J Cataract Refract Surg*. 2020;46:388–393.
39. Kohnen T, Böhm M, Hemkeppler E, et al. Visual performance of an extended depth of focus intraocular lens for treatment selection. *Eye (Lond)*. 2019;33:1556–1563.
40. Tan J, Qin Y, Wang C, Yuan S, Ye J. Visual quality and performance following bilateral implantation of TECNIS Symfony intraocular lenses with or without micro-monovision. *Clin Ophthalmol*. 2019;13:1071–1077.
41. Ruiz-Mesa R, Abengózar-Vela A, Aramburu A, et al. Comparison of visual outcomes after bilateral implantation of extended range of vision and trifocal intraocular lenses. *Eur J Ophthalmol*. 2017;27:460–465.
42. Gatinel D, Loicq J. Clinically relevant optical properties of bifocal, trifocal, and extended depth of focus intraocular lenses. *J Refract Surg*. 2016;32:273–280.
43. Zapata-Díaz JF, Rodríguez-Izquierdo MA, Ould-Amer N, Lajara-Blesa J, López-Gil N. Total depth of focus of five premium multifocal intraocular lenses. *J Refract Surg*. 2020;36:578–584.
44. Lee Y, Łabuz G, Son HS, Yildirim TM, Khoramnia R, Auffarth GU. Assessment of the image quality of extended depth-of-focus intraocular lens models in polychromatic light. *J Cataract Refract Surg*. 2020;46:108–115.
45. Domínguez-Vicent A, Esteve-Taboada JJ, Del Águila-Carrasco AJ, Ferrer-Blasco T, Montés-Micó R. In vitro optical quality comparison between the Mini WELL Ready progressive multifocal and the TECNIS Symfony. *Graefes Arch Clin Exp Ophthalmol*. 2016;254:1387–1397.
46. Chae SH, Son HS, Khoramnia R, Lee KH, Choi CY. Laboratory evaluation of the optical properties of two extended-depth-of-focus intraocular lenses. *BMC Ophthalmol*. 2020;20:53.
47. Lamba A, Pereira A, Varma D, Shahidi A, Smith D, Ahmed IIK. Retrospective analysis on the visual outcomes and photic phenomena following bilateral extended depth of focus intraocular lens implants. *Can J Ophthalmol*. 2020;55:126–130.
48. Hammond MD, Potvin R. Visual outcomes, visual quality and patient satisfaction: comparing a blended bifocal approach to bilateral extended depth of focus intraocular lens implantation. *Clin Ophthalmol*. 2019;13:2325–2332.
49. Sachdev GS, Ramamurthy S, Sharma U, Dandapani R. Visual outcomes of patients bilaterally implanted with the extended range of vision intraocular lens: a prospective study. *Indian J Ophthalmol*. 2018;66:407–410.
50. Hwang HS, Park SK, Kim MS. The biomechanical properties of the cornea and anterior segment parameters. *BMC Ophthalmol*. 2013;13:49.
51. Richdale KL, Jones LA, Mitchell GL, Zadnik K, Mutti DO, Bullimore MA. Crystalline lens thickness from infancy to adulthood. *Invest Ophthalmol Vis Sci*. 2008;49:3137–3137.
52. Cinar E, Bolu H, Erbakan G, et al. Vision outcomes with a new monofocal IOL. *Int Ophthalmol*. 2021;41:491–498.
53. Webster MA, Georgeson MA, Webster SM. Neural adjustments to image blur. *Nat Neurosci*. 2002;5:839–840.
54. Na KS, Kim SJ, Nam G, et al. A novel intraocular lens simulator that allows patients to experience the world through multifocal intraocular lenses before surgeries. *Transl Vis Sci Technol*. 2022;11(3):14.

Supplementary Material

Supplementary Movie S1. Focusing with monofocal IOL. With monofocal IOL, the letters on the signboard were clearly visible when the focus was on the focal plane of an objective lens. However, they became blurry as the focus passed the focal plane of the objective lens.

Supplementary Movie S2. Focusing with Eyhance. With Eyhance, when the far focus was on the focal plane of the objective lens, the image was clear. As the cornea- intraocular lens complex approached the objective lens, the image became slightly blurry. Then, it became slightly clearer again. At this time, a halo was observed around the street lamp, which was small (diameter: 60 pixels) but strong.

Supplementary Movie S3. Focusing with bifocal IOL. With the bifocal IOL, the image was hazy and foggy compared to the monofocal IOL when the first (far) focus is on the focal plane of the objective lens, and the halo (diameter: 171 pixels) is observed around the street lamp. As the cornea-IOL complex approached the focal plane of the objective lens, the image became significantly blurry. Then, it became clear again when the second (near) focus was on the objective lens. At this time, the halo (diameter: 203 pixels) was observed around the street lamp.

Supplementary Movie S4. Focusing with Symfony. With Symfony, the image is hazy and foggy compared to that with the monofocal IOL. The halo (diameter: 81 pixels) was observed around the street lamp. As the cornea-IOL complex approached the focal plane of the objective lens, the image became blurry. Then, it became clear again when the second (near) focus was on the objective lens. The halo (diameter: 85 pixels) around the street lamp at the second focus was slightly weaker than that at the first focus. The two foci were significantly closer compared to the foci in the bifocal IOL. The images were not very blurry in this interval compared to the bifocal IOL.

Supplementary Movie S5. 6 m distance USAF 1951 resolution target with monofocal IOL. With the monofocal IOL, the image was significantly clear at 6 m. However, it blurred as the model eye approached the resolution target.

Supplementary Movie S6. 6 m distance USAF 1951 resolution target with Eyhance. With Eyhance, the image appeared slightly more blurred than the monofocal IOL at 6 m. As it approached the resolution target, it blurred. However, at 80 to 155 cm, the image looked clearer than that by the monofocal IOL.

Supplementary Movie S7. A 6 m distance USAF 1951 resolution target with bifocal IOL. With the bifocal IOL, the image was hazy compared to that with the monofocal IOL at 6 m. As it got closer, it blurred considerably. Then, it became clear again at approximately 50-60 cm. After that, the clarity decreased as the distance decreased.

Supplementary Movie S8. A 6 m distance USAF 1951 resolution target with Symfony. With Symfony, the image was hazier compared to that with the monofocal IOL at 6 m. As the distance between them decreased, the image blurred. Then, it became clear again at approximately 90 to 110 cm. After that, the clarity decreased as the distance decreased.

Supplementary Movie S9. Night street with monofocal IOL. With the monofocal IOL, the pixels looked rough compared to the daytime. However, there was no definite halo around the headlights, tail lights of the cars, and traffic lights.

Supplementary Movie S10. Night street with Eyhance. Eyhance is similar to the monofocal IOL. However, there are few small halos (75 pixels) around street lamps compared to monofocal IOL (52 pixels).

Supplementary Movie S11. Night street with bifocal IOL. In the image with the bifocal intraocular lens, the halo around the headlights, tail lights of the cars, and traffic lights, and street lamps (185 pixels) were definite and large compared to the monofocal IOL.

Supplementary Movie S12. Night street with Symfony. Symfony is similar to the bifocal IOL. However, the size of the halo (street lamp: 85 pixels) was smaller than that of the bifocal IOL.